Study of quantum effects on atomic displacements in quartz

doi: 10.1016/j.jpcs.2010.05.010

Study of quantum effects on atomic displacements in quartz

H. Fujishita[a,b,1], M. Hayashi[b], T. Kanai[b], T. Yamada[b], N. Igawa[c], K. Kihara[d]

[a] School of Mathematics and Physics, Kanazawa University, Kanazawa, 920-1192, Japan
[b] Division of Mathematical and Physical Sciences, Kanazawa University, Kanazawa, 920-1192, Japan
[c] Quantum Beam Science Directorate, Japan Atomic Energy Agency, Tokai-mura, Naka-gun, Ibaraki 319-1195, Japan
[d] School of Natural Systems, Kanazawa University, Kanazawa 920-1192, Japan

Abstract

The crystal structure of quartz (SiO_2) was analyzed by neutron powder diffraction at several temperatures in the range of 10–250 K. The temperature dependence of the structure parameters was consistent with our previous results obtained using single-crystal X-ray diffraction above room temperature. Atomic displacements are order parameters for displacive structural phase transitions. The temperature evolution of Si atomic displacement in quartz was analyzed by studying the quantum expansion of the Landau potential. The expansion was found to accurately describe the evolution of the atomic displacement over the entire temperature interval. To the best of our knowledge, such a verification of atomic displacement is the first of its kind. A proportional relationship between spontaneous strain and the square of the atomic displacement was observed over the entire temperature interval. The validity of the obtained characteristic temperature for the quantum effect is discussed and compared with the results of previous Raman-scattering studies.

Key words: A. oxides; C. neutron scattering; D. crystal structure; D. phase transitions; D. thermodynamic properties

1. Introduction

It is well known that order parameter Q corresponds to atomic displacements in displacive structural phase transitions. These transitions are caused by the condensation of some unstable lattice vibrational modes. A phenomenological theory with a Landau potential describes the temperature dependence of the order parameter near a phase transition, except at the critical region. The theory also describes the temperature dependence of spontaneous strain if the coupling between the order parameter and the strain e (i.e., secondary order parameter) is taken into account. Analyses based on this classical phenomenological theory have been applied extensively to many structural phase transitions. In previous research, we performed a precise X-ray structure analysis of quartz (SiO_2), which undergoes a structural phase transition near 846K, at various temperatures above 298K [1]. The results indicated that above 298K, the Si atom displacement in quartz and the lattice parameter variations obey the classical phenomenological theory [2].

However, this classical theory cannot describe the temperature dependence of the order parameter at low temperatures because of the quantum effect. Salje et al. derived the quantum expression of the Gibbs free energy as follows [3, 4]:

$$G(Q,T) = G_0(T) + \frac{1}{2}A\Theta_s[coth(\Theta_s/T) - coth(\Theta_s/T_0)]Q^2 + \frac{1}{4}BQ^4 + \frac{1}{6}CQ^6, \quad (1)$$

where T is temperature and $k_B\Theta_s = \hbar\Omega_0/2$ with Ω_0 being the local frequency for small oscillations in the absence of interactions. The quantities A, B, and C are temperature-independent coefficients, with A and C always positive. T_0 is the temperature at which the coefficient of Q^2 in equation (1) changes its sign. When $B \geq 0$, a continuous phase transition occurs at T_0. The transition exhibits a tricritical behavior when $B = 0$. A first-order phase transition with the *thermodynamic* transition temperature $T_c = T_0 + 3B^2/(16AC)$ occurs when $B < 0$. The classical Landau potential follows as a high-temperature approximation of equation (1) when T and $T_0 \gg \Theta_s$, making it possible to examine the temperature dependence of the order parameter over the entire temperature interval. By introducing a coupling term $-DeQ^2$ and an elastic term $Ke^2/2$ to equation (1), we obtain the following relationship between the strain and order parameter from an equilibrium condition for strain:

$$e = \left(\frac{D}{K}\right)Q^2, \quad (2)$$

where D and K are a temperature-independent coupling constant and an elastic constant ($D, K > 0$), respectively. In terms of a low-temperature phase lattice parameter a_{LT} and a high-temperature phase lattice parameter a_{HT} that is extrapolated to the same low temperature (i.e., a hypothetical lattice parameter of high-temperature phase at a low temperature), the spontaneous strain is defined as follows [5]:

$$e_a = (a_{LT} - a_{HT})/a_{HT}. \quad (3)$$

By substituting equation (2) into the coupling and elastic terms, we obtain the temperature dependence of the square of the order

Email address: fujishit@kenroku.kanazawa-u.ac.jp (H. Fujishita)

parameter below the transition temperature from an equilibrium condition for the order parameter:

$$Q^2 = -\frac{B}{2C} + \sqrt{\frac{A}{C}\Theta_s\left(coth\left(\Theta_s/T_0\right) - coth\left(\Theta_s/T\right)\right) + \left(\frac{B}{2C}\right)^2}, \quad (4)$$

where the coefficient of Q^4 in the Landau potential, $B - D^2/2K$, is written as B again for simplicity.

The temperature dependence of the order parameters for $B > 0$ and $B = 0$ was compared with the following experimental results obtained between the transition temperature and low temperature [3, 4]. The spontaneous strain in $Ca_{0.98}Na_{0.02}Al_{1.98}Si_{2.02}O_8$ ($B > 0$), axial splitting D of Fe^{3+} EPR spectrum of $LaAlO_3$ ($B > 0$), spontaneous strain in $NaNO_3$ ($B = 0$), and birefringence in $Pb_3(PO_4)^2$ ($B = 0$) [3, 4]. Recently, lattice-parameter measurements of SiO_2 have been performed in the temperature range of 10–900 K [6, 7], and spontaneous strains along the a and c directions were shown to follow equation (4) for $B = 0$ [7].

The applicability of equation (4) has been thus examined mainly via secondary order parameters though coupling with the order parameters. To our knowledge, thus far, no studies have been investigated the temperature dependence of the order parameter by analyzing atomic displacements over the entire temperature interval below T_c. However, such an analysis is desirable because atomic displacements are actually the order parameter Q in displacive structural phase transitions. The phase transition of SiO_2 from the high-temperature hexagonal phase to the low-temperature trigonal phase is suitable for this purpose because the precise structure analyses using anisotropic thermal parameters have already been carried out between 298K and 1126 K [1]. In addition, in the high-temperature phase, the softening of the silent mode at the Γ point is directly observed by hyper-Raman scattering. The square of the frequency exhibits a linear temperature dependence, which indicates that the phase transition is displacive [8]. Precise structure analyses using anisotropic thermal parameters between room temperature and zero temperature to examine the temperature dependence of order parameter by atomic displacements over the entire temperature interval below T_c have not been carried out. Therefore, we carried out a precise structure analysis of quartz by neutron powder diffraction in the temperature range of 10–250 K.

2. Experimental details

Single crystals of quartz were supplied by Nihon Dempa Kogyo Co., Ltd. The crystals were crushed and then ground finely in an aluminum mortar. We passed the resulting powder through a sieve with an opening of 63 μm to reduce any preferred orientation effect.

Powder neutron diffraction patterns of quartz at 10, 50, 100, 150, 200, and 250 K were obtained using a high-resolution powder diffractometer (HRPD) installed at JRR-3M in JAEA. This diffractometer uses 64 detectors, and the angles between the detectors are 2.5°. The incident neutron wavelength was 1.8228 Å, and collimation was 6'-40'-6'. The powder specimen was mounted to the HRPD apparatus and placed in a refrigerator with a closed-cycle He gas system. The specimen temperature was controlled to within ±0.1 K. A 10-mm-diameter vanadium sample cell was used to avoid diffraction peaks from the cell. Intensity data were collected by the scan of the counter system at 0.05° steps (2θ) during the angle of 2.5°.

Diffraction patterns between 10° and 150° were analyzed by the Rietveld method using the computer program RIETAN-2000 [9]. The scattering lengths were 4.149×10^{-13} cm and 5.803×10^{-13} cm for Si and O, respectively. The background level was fit by a polynomial expression. A pseudo-Voigt function was applied to the profile of powder neutron diffraction peaks, and a conjugate direction method was employed in the least-squares refinements. Application of equation (4) to the temperature dependence of atomic displacements was done using the computer program KaleidaGraph.

3. Results

The resulting neutron powder diffraction patterns were analyzed based on the trigonal space group $P3_221$- D_3^6 (No. 154) [1], where Si atoms are at the special positions $3a$ (x, 0, 2/3) and O atoms are at the general positions $6c$ (x, y, z). The $3a$ and $6c$ designations are the Wyckoff letters with multiplicities. We adopted anisotropic thermal parameters U_{ij} for both Si and O atoms. The relationships $U_{12} = U_{22}/2$ and $U_{13} = U_{23}/2$ exist for Si atoms, because they occupy the $3a$ sites. Results of the profile fit are shown in Figure 1; the number of reflections is 66. Structure parameters, lattice parameters, and the R factors of each fit are listed in Table 1.

Figure 2 shows the temperature dependence of lattice parameters and Figure 3 shows the temperature dependence of atomic displacements from their high-temperature positions in fractional coordinates. These figures also include our previous data to show the temperature dependence over the entire temperature interval. All temperature dependences show a smooth transition in the low-temperature phase.

To emphasize the nearly tricritical behavior of the transition, the fourth power of the displacement of the Si atom, Δx^4(Si), along the a direction from its high-temperature position is shown as a function of temperature in Figure 4. The square of the change of the lattice parameter a from the high-temperature value, Δa^2, is also shown in Figure 4 to provide a comparison with Δx^4(Si), where the high-temperature value is taken to be independent of temperature. The scale of Δa^2 is adjusted so that it matches the value of Δx^4(Si) at 10 K. The result of a least-squares fitting of equation (4) to Δx^2(Si) is shown by the solid line in Figure 4. The results for T_c, T_0 and Θ_s are 835 K ± 4 K, 817 K ± 7 K and 137 K ± 26 K, respectively, where the errors are standard errors. The coefficient of determination R^2 for this fit is 0.999.

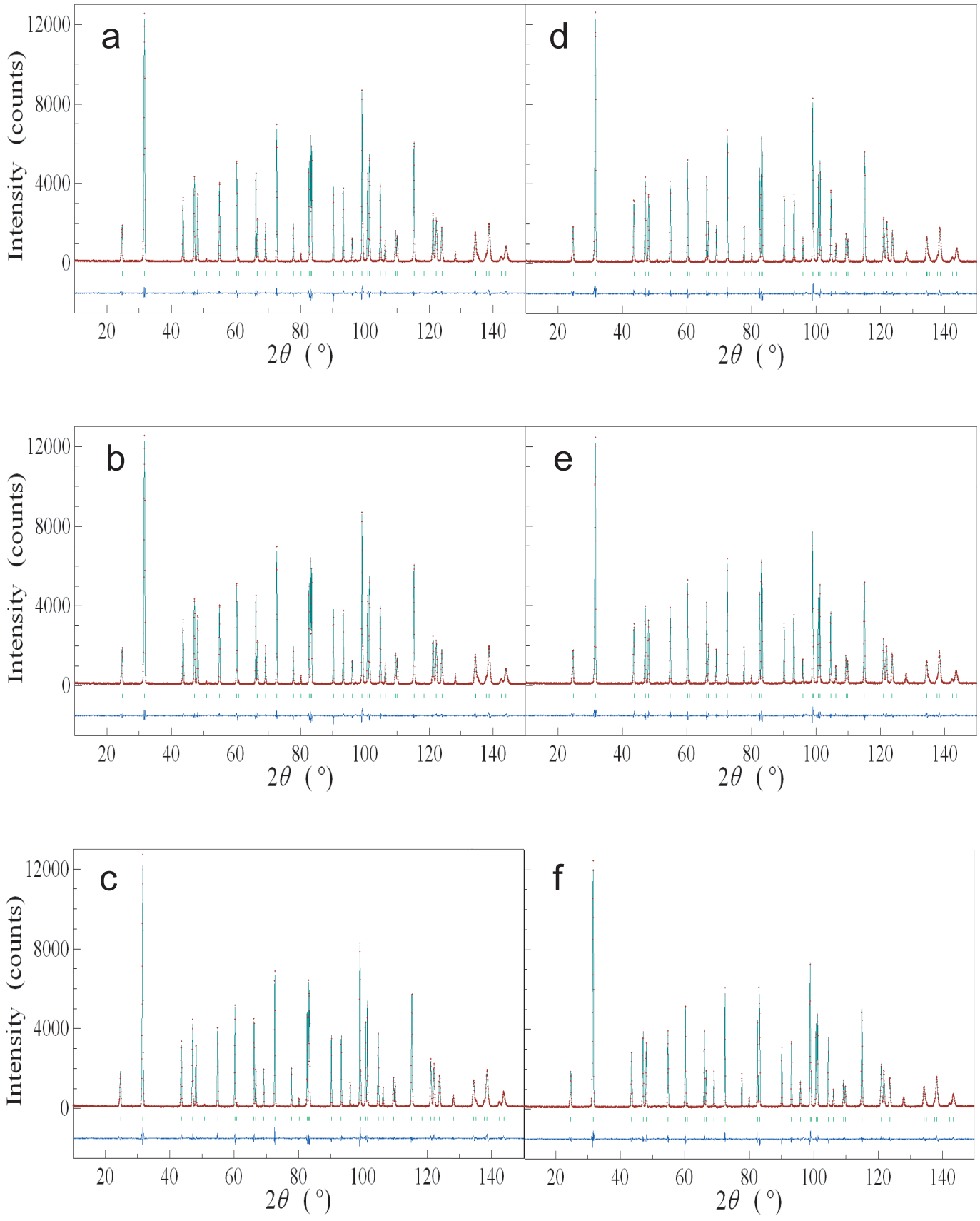

Figure 1: Neutron Rietveld refinement patterns for quartz at (a) 10, (b) 50, (c) 100, (d) 150, (e) 200, and (f) 250 K. The incident wavelength was 1.8228 Å. Calculated patterns are denoted by green lines passing though red data points in the upper portions. Short vertical green bars below the patterns indicate the positions of 66 allowed reflections. The blue lines in the lower portions show differences between the observed and the calculated patterns.

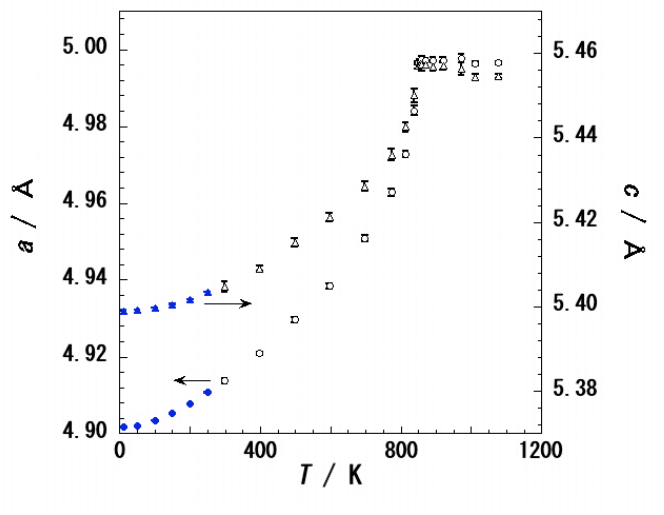

Figure 2: Temperature dependences of lattice parameters a of quartz (left hand scale; circles) and c (right hand scale; triangles). Our previous results obtained above room temperature [1] are indicated by open symbols to show the temperature dependence over the entire temperature interval.

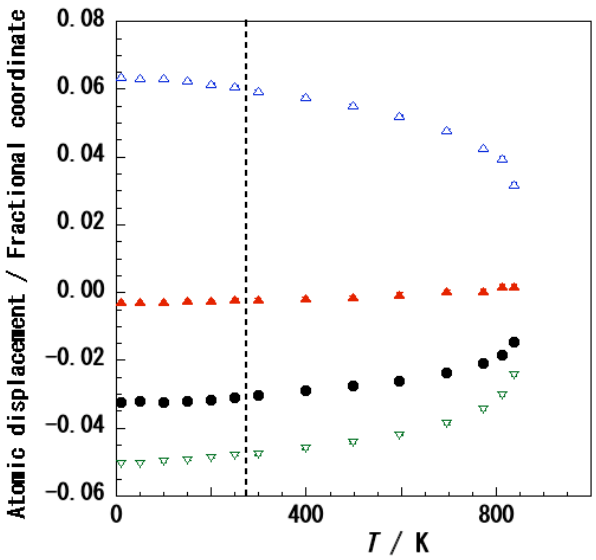

Figure 3: Temperature dependence of displacements of Si and O atoms of quartz from their high-temperature positions, in fractional coordinates. The vertical broken line indicates the boundary between the present results (low-temperature side) and our previous results [1] (high-temperature side). Δx(Si): circles; Δx(O): closed triangles; Δy(O): open triangles; Δz(O): open inverted triangles.

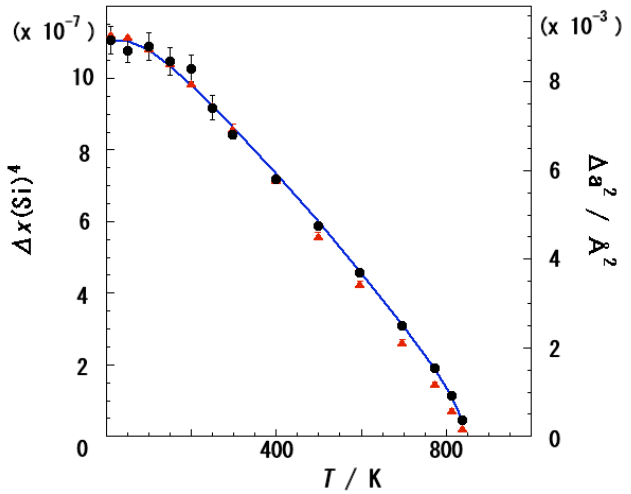

Figure 4: Fourth power of displacement of Si atom from its high-temperature position along a direction, Δx^4(Si), as a function of temperature (left ordinate; circles). The solid line shows the least-squares fit of the phenomenological relationship to Δx^4(Si). The right ordinate shows the square of change in lattice parameter a from its high-temperature value (triangles).

4. Discussions

4.1. Structure analysis

The resulting structure parameters of quartz are consistent from those obtained with our previous structure (i.e., the end-point values of the temperature-dependence curves agree). The following requirements are known to apply to anisotropic thermal parameters β_{ij} [10]:

$\beta_{ii} > 0, \beta_{ii}\beta_{jj} - \beta_{ij}^2 > 0$ for $i \neq j$, and $det\boldsymbol{\beta} > 0$,

where $\beta_{ij} = 2\pi^2 a_i^* a_j^* U_{ij}$, with $\boldsymbol{\beta}$ being a 3×3 matrix whose element ij is β_{ij}, and the a_i^* values are reciprocal lattice parameters without the factor 2π. The anisotropic thermal parameters satisfy these requirements except those at 10 and 50 K, where the value of $\beta_{11}\beta_{22} - \beta_{12}^2$ and of $det\boldsymbol{\beta}$ for Si at 10 and 50 K are slightly negative values. However, we consider the thermal parameters obtained to be essentially correct because the error in the term $\beta_{11}\beta_{22} - \beta_{12}^2$ is about twice as large as $|\beta_{11}\beta_{22} - \beta_{12}^2|$ and the error in $det\boldsymbol{\beta}$ is about five times larger than $|det\boldsymbol{\beta}|$.

Upon increasing the temperature above room temperature, the Si and O atoms move along a line toward their high-temperature-phase positions. For Si atoms, the lines are coincident with the two-fold axes along ⟨100⟩. For O atoms, the lines make constant angles of about 41° to 42° with [010] on {100} [1]. The O position is shown in Figure 5 as a function of temperature. For the low-temperature phase, and for temperatures above room temperature, the data are shown by open circles with a dot. The present results, which are also for the low-temperature phase, but for temperatures below room temperature, are shown by open circles. For the high-temperature phase, the O position is shown by filled circles and shows no significant change with temperature.

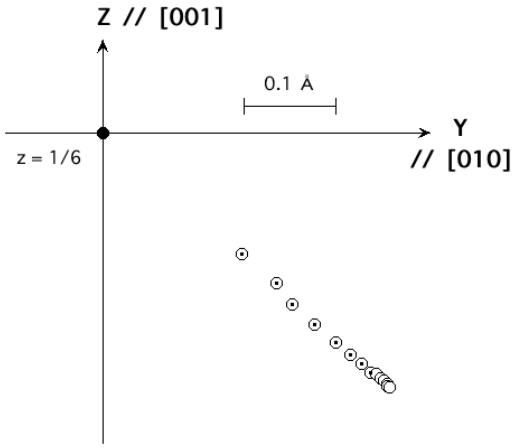

Figure 5: [210] projection (i.e., projection on *bc*-plane) of O atom at different temperatures. Positions in the low-temperature phase are indicated by circles with dot (above room temperature) or open circles (below room temperature). Full circles indicates the positions in the high-temperature phase.

4.2. Atomic displacement, spontaneous strain, and the quantum effect

We fit the square of phenomenological temperature evolution of the order parameter to the square of the Si atom displacement over the entire temperature interval. The observed temperature evolution was obtained by combining the present structure analysis (below 250K) with our previous structure analysis (above 298K). The fit indicates that quantum expansion of the phenomenological theory can describe the behavior of order parameter quite well over the entire temperature interval, as shown by the solid line in Figure 4. We have thus accurately described the atomic displacement, which is the order parameter itself, over the entire temperature range.

Spontaneous strain e_a along the a direction is defined by equation (3) using a hypothetical lattice parameter a_{HT} for the high-temperature phase at a low temperature. We can consider a_{HT} for quartz to be independent of temperature because the lattice parameter a exhibits only a slight temperature dependence in the high-temperature phase [1, 6, 7], as shown in Figure 2. In this case, we can treat e_a as proportional to $\Delta a = a_{LT} - a_{HT}$. The plot of $\Delta a^2 (\propto e_a^2)$ is shown in Figure 4. We can see that the relationship $e_a^2 \propto \Delta x^4$(Si) (i.e., the square of equation (2)), holds over the entire temperature interval.

From the present analysis of the atomic displacement, we find a characteristic temperature Θ_s of 137 ± 26 K, which corresponds to the temperature of the zero-point local frequency for small oscillations in the absence of interactions. The value previously obtained from analyzing the spontaneous strain, for which the phase transition was treated as tricritical, is 187 K [7]. The difference between these values is not significant, because the error for the previously reported value was not reported and the difference is within twice the error of the current study. However, these temperatures seem too large to be the actual characteristic temperature for the quantum effect.

Therefore, we examine the validity of the temperature in connection with soft-mode condensation. A soft-mode condensation with high damping is clearly observed by hyper-Raman scattering in the high-temperature phase of quartz, and a linear dependence of the square of the frequency on temperature was detected until very close to the transition temperature [8]. A nonlinear interaction exists between the soft mode and a mode generated by two zone boundary acoustic modes in the low-temperature phase [11]. This interaction causes an anticrossing of these modes around 550 K. A linear dependence on temperature of the square of the soft-mode frequency is expected in the absence of this interaction in the low-temperature phase; the wave number of the soft mode at absolute zero is estimated to be 240 cm^{-1} [11]. Because the temperature Θ_s that corresponds to 240 cm^{-1} is 170 K, we consider the experimentally obtained values to be reasonable.

5. Conclusions

We successfully analyzed the structure of quartz using neutron powder diffraction at several temperatures between 10 K and 250 K and analyzed the temperature evolution of Si atomic displacement by studying the quantum expansion of the Landau potential. The expansion accurately describes the temperature dependence over the entire temperature interval. We also observed a proportional relationship between spontaneous strain and the square of the atomic displacement over the entire temperature interval.

6. Acknowledgements

We are grateful to Nihon Dempa Kogyo Co., Ltd., for providing the single crystals of quartz. This work was performed under the Common-Use Facility Program of JAEA.

References

[1] K. Kihara, Eur. J. Mineral. 2 (1990) 63.
[2] K. Kihara, J. Crystallogr. Soc. Jpn. 43 (2001) 218 (in Japanese).
[3] E.H.K. Salje, B. Wruck, H. Thomas, Z. Phys. B 82 (1991) 399.
[4] E.H.K. Salje, Acta Cryst. A 47 (1991) 453.
[5] E.H.K. Salje, Phase Transitions in Ferroelectric and Co-elastic Crystals, student ed., Cambridge University Press, Cambridge, 1993, p. 22.
[6] M.A. Carpenter, E.H.K. Salje, A. Graeme-Barber, B. Wruck, M.T. Dove, K.S. Knight, Am. Mineral. 83 (1998) 2.
[7] F.J. Romero, E.K.H. Salje, J. Phys. Condens. Matter 15 (2003) 315.
[8] Y. Tezuka, S. Shin, M. Ishigame, Phys. Rev. Lett. 66 (1991) 2356.
[9] F. Izumi, T. Ikeda, Mater. Sci. Forum 321-324 (2000) 198.
[10] C.K. Johnson, H.A. Levy, in: J.A. Ibers, W.C. Hamilton (Eds.), International Tables for X-ray Crystallography, vol. IV, Kynoch Press, Birmingham, 1974, p. 315.
[11] J. F. Scott, Phys. Rev. Lett. 21 (1965) 907.

Table 1: Positional parameters of Si and O atoms in fractional coordinates, their anisotropic thermal parameters U^a_{ij}, and lattice parameters at various temperatures of quartz obtained by powder neutron diffraction.

Structural parameters or R factors	Temperature					
	10 K	50 K	100 K	150 K	200 K	250 K
x(Si)	0.4676(3)	0.4678(3)	0.4677(3)	0.4680(3)	0.4682(3)	0.4691(3)
U_{11}(Si)	0.05(6)	0.08(5)	0.24(6)	0.34(6)	0.39(6)	0.58(7)
U_{22}(Si)	0.56(10)	0.55(9)	0.74(11)	0.73(11)	0.94(11)	0.94(11)
U_{33}(Si)	0.27(10)	0.30(9)	0.44(11)	0.43(11)	0.53(12)	0.67(12)
U_{23}(Si)	0.16(7)	0.14(6)	0.10(7)	0.19(8)	0.13(8)	0.10(8)
U_{eq}(Si)	0.24	0.26	0.42	0.46	0.56	0.69
x(O)	0.4126(2)	0.4128(2)	0.4126(2)	0.4130(2)	0.4129(2)	0.4135(2)
y(O)	0.2714(2)	0.2711(2)	0.2710(2)	0.2702(2)	0.2694(2)	0.2687(2)
z(O)	0.7827(2)	0.7828(1)	0.7833(2)	0.7839(2)	0.7844(2)	0.7852(2)
U_{11}(O)	0.44(5)	0.51(4)	0.71(5)	0.86(5)	1.14(5)	1.34(5)
U_{22}(O)	0.45(4)	0.48(4)	0.66(4)	0.77(4)	0.93(4)	1.07(4)
U_{33}(O)	0.26(4)	0.29(4)	0.46(4)	0.58(4)	0.73(4)	0.88(5)
U_{12}(O)	0.32(4)	0.32(4)	0.44(4)	0.56(4)	0.71(4)	0.89(4)
U_{13}(O)	-0.02(3)	-0.02(3)	-0.06(3)	-0.10(4)	-0.14(4)	-0.15(4)
U_{23}(O)	0.03(3)	-0.03(3)	0.02(3)	-0.09(4)	-0.12(4)	-0.15(4)
U_{eq}(O)	0.35	0.40	0.57	0.67	0.85	0.97
a (Å)	4.90179(8)	4.90198(8)	4.90338(9)	4.90520(9)	4.90772(9)	4.91067(9)
c (Å)	5.39914(7)	5.39922(6)	5.39981(7)	5.40060(7)	5.40182(7)	5.40355(7)
V (Å^3)	112.347(4)	112.358(3)	112.435(4)	112.535(4)	112.676(4)	112.847(4)
R_{wp} (%)	7.36	6.62	7.51	7.42	7.35	7.23
R_p (%)	5.32	4.69	5.50	5.45	5.28	5.22
R_F (%)	0.91	0.94	1.07	0.91	0.96	1.09
R_I (%)	1.55	1.59	1.77	1.52	1.60	1.68

The space group is $P3_221$ - D^6_3 (No. 154). Si and O atoms are at the 3a and 6c positions, respectively, where y(Si) = 0.0, z(Si) = 2/3, U_{12}(Si) = U_{22}(Si)/2 and U_{13}(Si) = U_{23}(Si)/2. Unit of U is Å^2, but values are multiplied by 100. U_{eq} is the equivalent isotropic thermal parameter calculated from U_{ij}. Numbers in parentheses indicate the estimated standard deviations. R factors of each profile fit are also indicated.

[a] Temperature factor for each atom is expressed by U_{ij} as follows;

$$exp\Big[-2\pi^2(h^2a^{*2}U_{11} + k^2b^{*2}U_{22} + l^2c^{*2}U_{33} + 2hka^*b^*U_{12} + 2hla^*c^*U_{13} + 2klb^*c^*U_{23})\Big], \quad (5)$$

where a^*, b^*, and c^* are reciprocal lattice parameters without the factor 2π; and h, k, and l are Miller indices.